HHS Public Access

Author manuscript

Proc SPIE Int Soc Opt Eng. Author manuscript; available in PMC 2017 September 27.

Published in final edited form as:

Proc SPIE Int Soc Opt Eng. 2017 April ; 10133: . doi:10.1117/12.2254675.

Subject-Specific Longitudinal Shape Analysis by Coupling Spatiotemporal Shape Modeling with Medial Analysis

Sungmin Hong[a], **James Fishbaugh**[a], **Morteza Rezanejad**[b], **Kaleem Siddiqi**[b], **Hans Johnson**[c], **Jane Paulsen**[c], **Eun Young Kim**[c], and **Guido Gerig**[a]

[a]Computer Science and Engineering, Tandon School of Engineering, New York University

[b]School of Computer Science, McGill University

[c]Department of Psychiatry, Carver College of Medicine, University of Iowa

Abstract

Modeling subject-specific shape change is one of the most important challenges in longitudinal shape analysis of disease progression. Whereas anatomical change over time can be a function of normal aging; anatomy can also be impacted by disease related degeneration. Shape changes to anatomy may also be affected by external structural changes from neighboring structures, which may cause non-linear pose variations. In this paper, we propose a framework to analyze disease related shape changes by coupling extrinsic modeling of the ambient anatomical space via spatiotemporal deformations with intrinsic shape properties from medial surface analysis. We compare intrinsic shape properties of a subject-specific shape trajectory to a normative 4D shape atlas representing normal aging to separately quantify shape changes related to disease. The spatiotemporal shape modeling establishes inter/intra subject anatomical correspondence, which in turn enables comparisons between subjects and the 4D shape atlas, and also quantitative analysis of disease related shape change. The medial surface analysis captures intrinsic shape properties related to local patterns of deformation. The proposed framework simultaneously models extrinsic longitudinal shape changes in the ambient anatomical space, as well as intrinsic shape properties to give localized measurements of degeneration. Six high risk subjects and six controls are randomly sampled from a Huntington's disease image database for quantitative and qualitative comparison.

1. INTRODUCTION

Modeling subject-specific shape change is becoming possible through increased availability of repeated longitudinal scans of individual subjects.[1] In many clinical applications, longitudinal shape changes are not entirely explained by degeneration due to disease; changes are also impacted by normal aging. As an illustration, Figure 1 shows that high risk subjects of Huntington's disease(HD) have larger caudate degeneration rates across a large range of ages compared to controls. Shape changes of anatomy may not only be intrinsic but may also be affected by external structural changes from neighboring anatomies. For example, caudate and putamen of the basal ganglia are pushed outward by the expansion of the ventricles. Such external effects from other objects can cause non-linear variations of shapes in the pose of an anatomical structure, which can be coupled with intrinsic shape changes and thus complicate statistical analysis. Purely geometric shape changes are of

critical importance to measure atrophy or to localize degeneration. In this paper, we propose a framework to analyze disease related shape changes by coupling extrinsic modeling of the ambient anatomical space via spatiotemporal deformations[2] with intrinsic shape properties from medial surface analysis.[3]

Styner et al.[4] have estimated medial properties using a mesh of medial samples (m-reps) with fixed graph topology. Medial representations have thus far offered only an indirect method for 3D surface shape analysis since the correspondences are established between medial samples. Fishbaugh et al.[5] have analyzed shape variability over time by deformation on an ambient space. The intrinsic statistics of the deformation are computed in the ambient space which alleviates the need for explicit point correspondence between anatomical structures. However, the intrinsic shape change cannot be explicitly analyzed because it is coupled with pose variations. Younes et al.[6] have shown shape differences between risk groups of HD based on deformation to a template shape, but without considering longitudinal information.

We propose to determine subject-specific trajectories via spatiotemporal modeling, which establishes anatomical correspondence on the surface of the anatomical structures. This 4D deformation includes local deformation information and positional changes influenced by neighboring structures. We isolate local deformation properties with a medial surface representation, which provides an intrinsic measure of thickness which can be mapped to the structure's surface. We leverage the anatomical correspondence between shapes to make comparisons between subjects and a 4D atlas representing normal aging and to quantify shape changes related to disease. In this manner we capture extrinsic longitudinal shape changes which account for the interactions between multiple shapes, as well as intrinsic shape properties which give localized measurements of degeneration. Qualitative and quantitative assessments of subject-specific shape trajectories of six randomly sampled HD subjects and six controls demonstrate the potential of our method to capture longitudinal shape changes and disease related degeneration.

2. METHODS

We combine spatiotemporal modeling to capture subject-specific shape trajectories and a 4D normative shape atlas built from a normal aging population with medial surface analysis via Hamilton-Jacobi skeletonization. Intrinsic shape features, including medial surface radii, are assigned to the corresponding points on the structure's surface. We compare subject-specific shape trajectories to a 4D normative shape atlas to analyze disease related shape changes which are not explained by normal aging effects.

2.1 Shape Trajectory Comparison to 4D Normative Atlas

Rather than modeling each shape independently, we consider a single time-varying deformation of the ambient 3D space, with multiple shapes of interest embedded into the shared space. Each continuous and smooth subject-specific shape trajectory is estimated for each individual subject in the ambient 3D shape space over a time axis by utilizing an initial baseline shape and a few intermittent follow-up observations. The subject-specific shape trajectory represents a continuous time-varying deformation of shapes from the series of

observations over time in a range from an initial observation time-point to the last follow-up observation. Thus, shape changes associated with normal aging cannot be ignored because of the distribution of ages in our patient population (see Fig 1), a problem well described by Lorenzi et al.[7] To neutralize shape changes caused by normal aging and to analyze shape changes solely related to disease progression, we compare the subject-specific shape trajectories to a normative 4D shape atlas. We estimate a normative 4D shape atlas utilizing 243 observations of healthy subjects without risk of the disease from 23 to 88 years of age. The atlas provides a normative reference used to make meaningful comparisons between the subject-specific shape trajectories in the HD and control groups.

Both the normative 4D shape atlas and the subject-specific shape trajectories are estimated via a geodesic shape regression method[2] which will be elaborated in the following section. For both subject-specific models and atlas estimation, we start from a common parameterization for the baseline shape configuration. This allows us to define the number of shape points as well as connectivity, and importantly, provides correspondence assuming an appropriately dense sampling and that the shapes are anatomically similar. As illustrated in Figure 2, we compare a subject-specific shape trajectory to a part of the normative 4D shape atlas at a corresponding time range with given correspondence on shapes. For example, if a subject-specific shape trajectory is estimated by observations from age 63 to age 65, we compare the subject-specific shape trajectory to the part of the normative 4D shape atlas from age 63 to 65. Thus, by comparing the subject-specific shape trajectory to the corresponding part of the normative 4D shape atlas, shape changes caused by normal aging are taken out so that changes only caused by disease can be analyzed within each subject-specific shape trajectory.

2.2 Spatiotemporal Modeling

The time-varying deformation of both subject-specific shape trajectories and a normative 4D shape atlas is modeled as a geodesic flow of diffeomorphisms, which are smooth and invertible transformations of 3D space.[2] The geodesic shape regression model estimates a continuous shape trajectory by a single time-varying deformation of 3D ambient space from a set of observed shapes O_{t_i}, a set of intermittent time-indexed shape observations (consisting of multiple shapes per time point). An initial baseline shape X_0 of each individual subject is estimated by matching a smooth ellipsoid to an initial observation of each subject, O_{t_0}. The geodesic flow of diffeomorphic deformation ϕ_t for a continuous shape trajectory is estimated by optimizing the energy function which matches the deformation ϕ_t to follow-up observations O_{t_i} with viscosity regularizer.

$$E(X_0, \phi_t) = \sum_{i=1}^{N_{obs}} \|\phi_{t_i}(X_0) - O_{t_i}\|^2_{W*} + Reg(\phi_t) \quad (1)$$

where $\|\cdot\|^2_{W*}$ represents the squared distance defined on currents[8] and $Reg(\phi_t)$ is the measure of regularity term of ϕ_t. By optimizing Eq. 1, the baseline shape X_0 smoothly deforms over time t by ϕ_t by the regularization which enforces diffeomorphism. Correspondence of

landmark points for different subjects are determined by the matching in an embedding space, assuming that the shapes are anatomically similar. Shapes in the estimated shape trajectories and a normative atlas are spatially and temporally smooth by the diffeomorphic transformation. With the continuous 4D normative atlas, we can extract the part of the normative atlas which is within a same time range of an individual subject-specific shape trajectory for analysis as described in the previous section.

2.3 Hamilton-Jacobi Medial Surface Estimation

The medial surface of a shape in the estimated shape trajectory is computed by detecting shocks in Blum's grassfire flow[9] by combining a measure of the average outward flux of the vector field underlying the Hamiltonian system with a homotopy preserving thinning process.[3] The detected shocks are classified into medial surface points and non-medial surface points by the average of outward flux at points, see[3] for more details.

The medial surfaces are estimated independently for each single shape in a shape trajectory. With inter/intra subject landmark correspondences already established during the spatiotemporal model estimation, we can project the correspondences of the landmark points of the shape boundary to the medial surface. Therefore, even though there is no direct calculation of an explicit relationship between medial surfaces of a shape trajectory, we can obtain correpondences on medial surfaces projected from the correspondences of object boundaries. A shape in a shape trajectory at time t_i can be deformed to match a shape at time t_j by the deformation ϕ_{t_i,t_j} from geodesic shooting. A medial surface of each shape in a shape trajectory is estimated by Hamilton-Jacobi skeletonization ψ_{t_i} at a time point ψ_{t_i}. With the spatio-temporal analysis providing correspondences on the structure's surface, these can be transferred to the associated medial surface points. The correspondences are visualized via local patch labels having the same color and medial surface radii are assigned to their corresponding structure surface points. Figure 3 shows structures from the 4D normative shape atlas smoothly deformed over e by diffeomoec deforeions $\psi_{0,T}$ from time 0 to T with correspondences between structures at different time points and correspondences to their medial surfaes colored from red to blue by the indices of landmark points. The initial baseline shape and its corresponding medial surface at the first column of Figure 3 are overlayed in following subfigures as transparent grey to show how shape boundaries and their corresponding medial surfaces changes with increasing age.

3. EXPERIMENTAL RESULTS

In this section, we present qualitative and quantitative comparisons of subjects in the high risk HD group and a control group. For this feasibility study, we randomly sample six subjects from each group out of 102 subjects in a control group and 106 subjects in a high risk HD group, for a total of 12 subjects, and compare distribution of radii, extracted from respective skeletons of left caudates.

Figure 4 visualizes radii difference of a subject in each group on the caudate surface. Radii differences are measured by subtracting radii at landmark points of the subject from a normative shape sampled from the 4D atlas at the same time point. The figure shows that an HD subject's shape is generally thinner (red) than a healthy subject of corresponding age,

especially at the middle part of the caudate. We can observe local radii difference in Figure 4 which cannot be represented by global measurements, such as volumes. Figure 5 shows histograms of radii on each subject's surface (red) and the corresponding shape of the 4D shape atlas at the same time point (blue). Histograms are fit with a gamma distribution to highlight differences in radii distributions. A control subject in Figure 5(a) shows similar radii distribution to an age matched shape from the normative 4D atlas, with similar peak and variance but small contribution from individual differences to the norm, while a subject in high risk HD group in Figure 5(b) shows substantial difference in radii distributions with a larger proportion of thin parts. Figure 5(c) summarizes closeness of each group to the normative atlas, displaying a whisker box plot of earth mover's distances (EMD)[10] between histograms of subjects and age matched shapes from the 4D shape atlas. Results show that control group subjects have more similar distribution to the 4D shape atlas while high risk HD subjects depict much larger differences. Longitudinal EMD changes of all subjects are plotted in Figure 5(d). The plot illurstrates that EMD of high risk group subjects increases as subjects get older while EMD of control group subjects do not show a strong trend within the time intervals. The residual differences of EMD of control subjects can be explained by subject-wise differences to the normative 4D shape atlas but temporal courses do not exhibit a specific change pattern. On the other hand, the increase of EMD over time of high risk group HD subjects seems to indicate that, in addition to differences at the initial measurements, there are disease related temporal shape changes far beyond normal aging effects.

4. CONCLUSIONS

The proposed methodology makes use of an extrinsic longitudinal shape regression to capture shape evolution which properly accounts for interactions between neighboring structures, as well as intrinsic shape properties of individual objects captured by medial surface analysis. The combination of the spatio-temporal modeling of shapes to estimate a continuous trajectory of shapes from intermittent observations and the Hamilton-Jacobi skeletonization reveals analysis of shape properties of time-series longitudinal shape data which to our knowledge have not been reported. Qualitative and quantitative assessments of longitudinal HD subject data demonstrate the feasibility of the proposed shape analysis framework. There are limitations of the proposed method which has to be stated. Since we estimate medial surfaces independently from each single shape in a shape trajectory, there is no direct relationship between medial surfaces across time. Here, we establish this correspondence indirectly via geodesic regression of shape boundaries. In the future, we will investigate a joint 4D regression of object boundaries and associated skeletal surfaces. In addition to the current summary measures of radii distributions, we will develop statistics of localized shape changes. The proposed scheme will be tested on large cohort of longitudinal HD data with different risk status to explore the relationship between longitudinal shape change and disease progression.

Acknowledgments

This research was supported by NIH grants U01 NS082086, NS40068, NS050568 (PREDICTHD), U54 EB005149 (NA-MIC), NIH (NINDS; 5RO1NS040068, 5RO1NS054893) and the CHDI Foundation to Jane S Paulsen. We

thank the PREDICT-HD sites, the study participants the National Research Roster for HD patients and families, the Huntington Disease Society of America and the Huntington Study Group.

References

1. Gerig G, Fishbaugh J, Sadeghi N. Longitudinal modeling of appearance and shape and its potential for clinical use. Med Image Anal. Oct.2016 33:114–121. [PubMed: 27344938]
2. Fishbaugh, J., Prastawa, M., Gerig, G., Durrleman, S. Information Processing in Medical Imaging. Springer; 2013. Geodesic shape regression in the framework of currents; p. 718-729.
3. Siddiqi K, Bouix S, Tannenbaum A, Zucker SW. Hamilton-Jacobi Skeletons. International Journal of Computer Vision. 2002; 48(3):215–231.
4. Styner M, Gerig G, Lieberman J, Jones D, Weinberger D. Statistical shape analysis of neuroanatomical structures based on medial models. Medical Image Analysis. 2003; 7(3):207–220. Functional Imaging and Modeling of the Heart. [PubMed: 12946464]
5. Fishbaugh, J., Prastawa, M., Durrleman, S., Piven, J., Gerig, G. Analysis of Longitudinal Shape Variability via Subject Specific Growth Modeling. Springer Berlin Heidelberg; Berlin, Heidelberg: 2012. p. 731-738.
6. Younes L, Ratnanather JT, Brown T, Aylward E, Nopoulos P, Johnson H, Magnotta VA, Paulsen JS, Margolis RL, Albin RL, Miller MI, Ross CA. Regionally selective atrophy of subcortical structures in prodromal HD as revealed by statistical shape analysis. Hum Brain Mapp. Mar.2014 35:792–809. [PubMed: 23281100]
7. Lorenzi M, Pennec X, Frisoni GB, Ayache N. Disentangling normal aging from Alzheimer's disease in structural magnetic resonance images. Neurobiol Aging. Jan; 2015 36(Suppl 1):42–52. [PubMed: 25169677]
8. Durrleman S, Pennec X, Trouvé A, Ayache N. Statistical models of sets of curves and surfaces based on currents. Medical image analysis. 2009; 13(5):793–808. [PubMed: 19679507]
9. Blum H. Biological shape and visual science (Part I). Journal of theoretical Biology. 1973; 38(2): 205–287. [PubMed: 4689997]
10. Rubner Y, Tomasi C, Guibas LJ. The earth mover's distance as a metric for image retrieval. International journal of computer vision. 2000; 40(2):99–121.

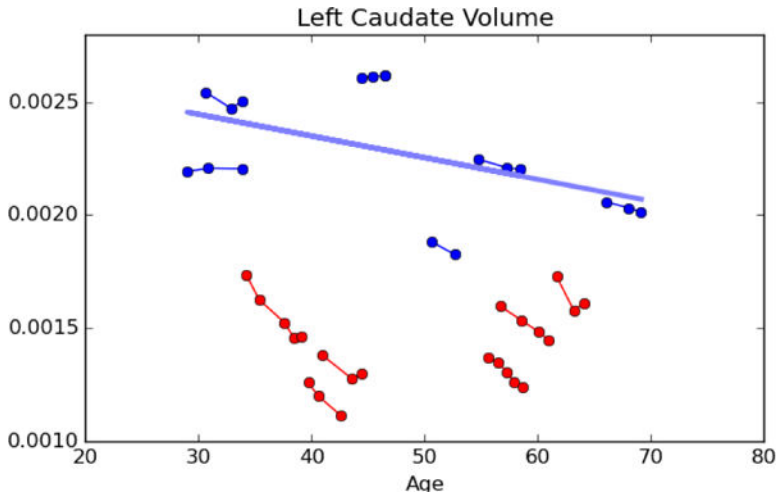

Figure 1.

Left caudate volume observations of subjects in a control group (blue) and a high risk group of Huntington's disease (red). The blue line shows linear regression of control group. HD subjects, regardless of age, show more rapid caudate degeneration.

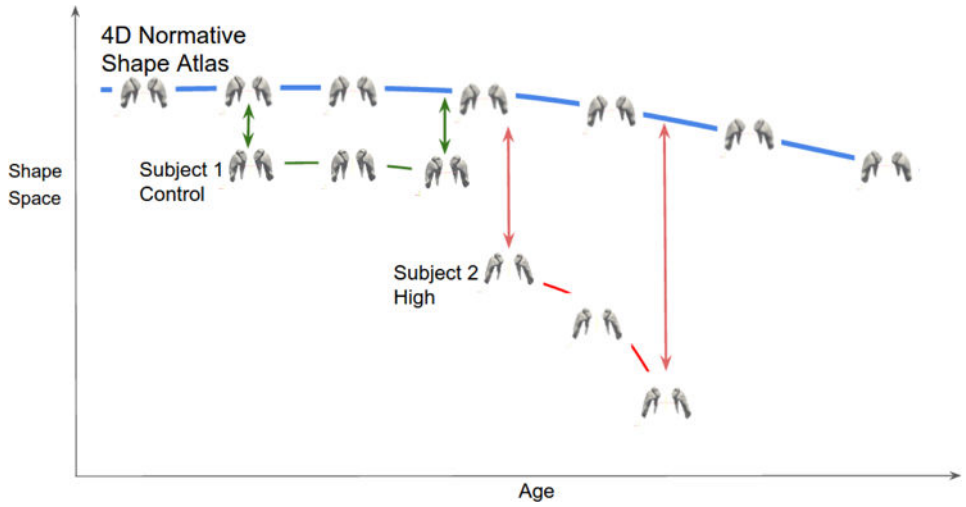

Figure 2.

An illustrative graph of shape comparison between a 4D normative shape atlas and subject-specific shape trajectories. Shape trajectories and a 4D atlas are estimated as a time-varying deformation of an ambient 3D shape space. Shapes in subject-specific shape trajectories either in HD (High risk) or control groups and the 4D atlas are in correspondence which enables to measure the shape difference in corresponding landmark points.

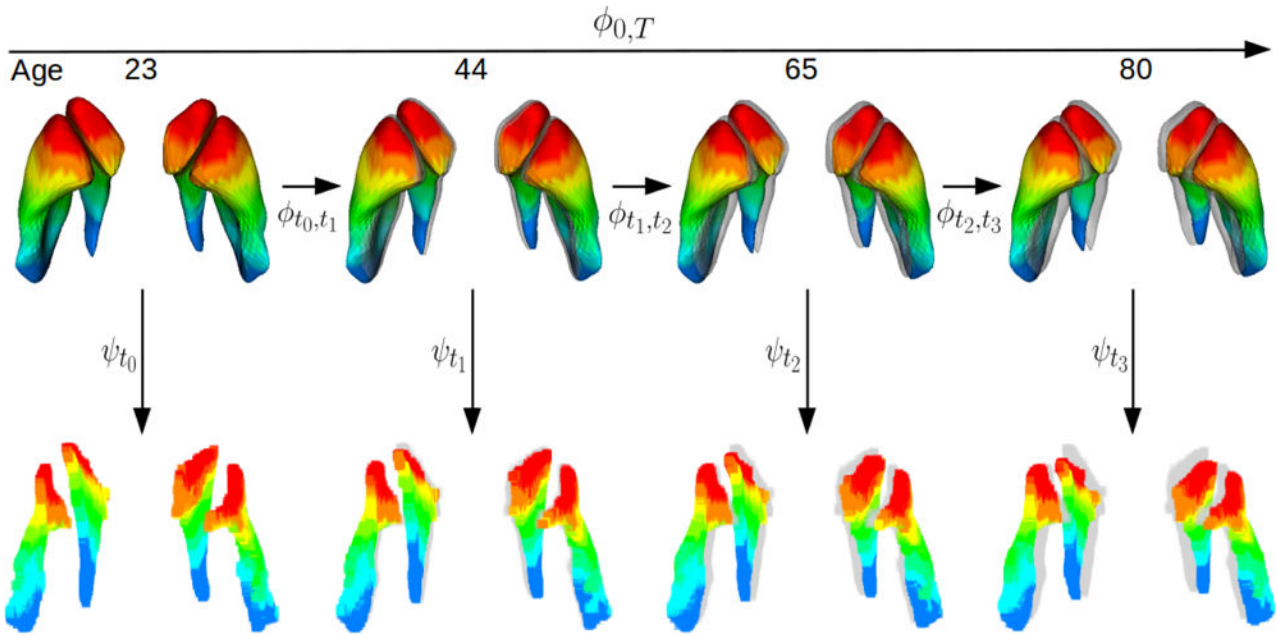

Figure 3.

Snapshots from the normative 4D shape atlas (top) and their medial surfaces with coloring of correspondence labels at 23, 44, 65 and 80 years of age. The 4D normative atlas is a continuous shape trajectory represented by the deformation $\phi_{0,T}$. Object boundaries in the atlas are diffeomorphic to each other by the spatiotemporal modeling bt ϕ_{t_i,t_j}. A medial surface at each time point is estimated independently from its object boundary at time point t_i via Hamilton-Jacobin skeletonization ψ_{t_i}. Medial surfaces are enhanced for a visualization purpose. The strcuture's surface at the initial time point (age 23) is overlayed in grey to show how the structures deform and are pushed outwards by normal aging over time.

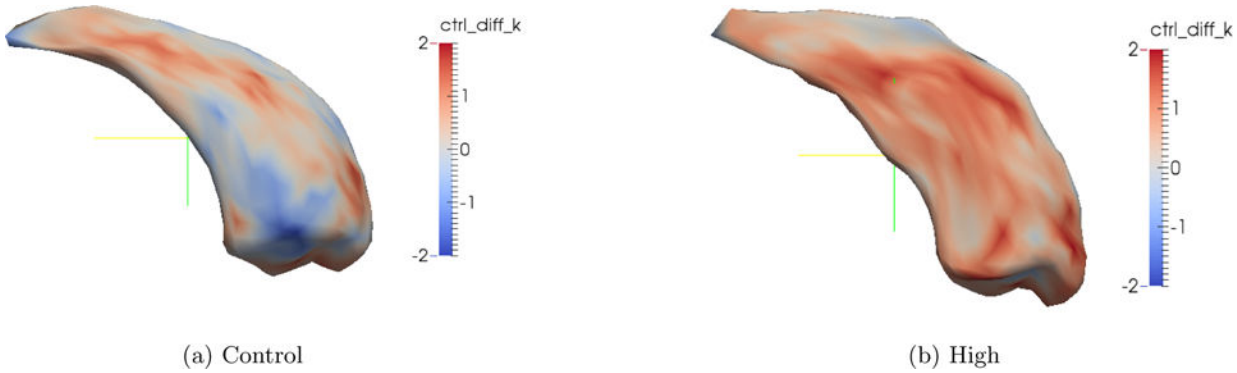

(a) Control (b) High

Figure 4.

Radii differences for the left caudate between an individual and the 4D shape atlas, projected from skeletons back to the object surfaces, of (a) a subject in a control group and (b) a subject in a high risk HD group. Red indicates regions that are thinner than a corresponding shape in the 4D shape atlas at the same time point while blue indicates regions that are thicker. Color bars on the right depict the range of radii differences (in mm units).

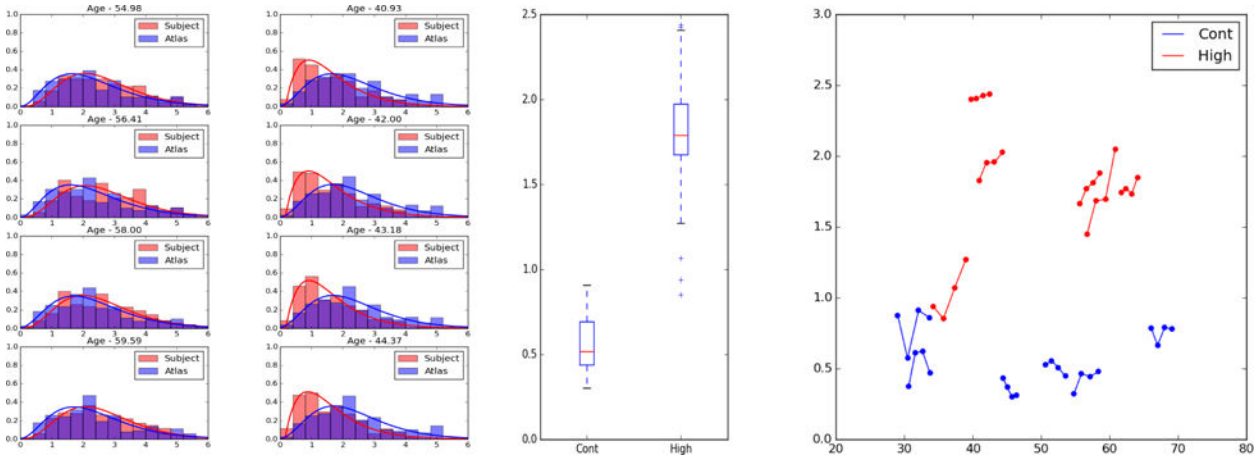

Figure 5.

Rows show different time points of a shape trajectory. (a,b) Histograms of radii distributions of subject-specific shape trajectories (red) of (a) a subject in a control group, (b) a subject in a high risk HD group compared to shapes of the 4D shape atlas at corresponding time points (blue) with fitted gamma distributions. (c) A whisker box plot of earth mover's distances (EMD) of all control group histograms and high risk HD group histograms to the 4D atlas. (d) Longitudinal EMD plots of subjects in a control group(blue) and a high risk HD group (red).